Shears mechanism in two-dimensional cranking relativistic mean field approach*

PENG Jing(彭婧)[1;1)] XING Li-Feng(邢丽峰)[1] MENG Jie(孟杰)[2,3,4]

1 (Department of Physics, Beijing Normal University, Beijing 100875, China)
2 (School of Physics, and SK Lab. of Nucl. Phys. & Tech., Peking University, Beijing 100871, China)
3 (Institute of Theoretical Physics, Chinese Academy of Sciences, Beijing,100080, China)
4 (Center of Theoretical Nuclear Physics, National Laboratory of Heavy Ion Accelerator, Lanzhou 730000, China)

Abstract Using the new two-dimensional cranking relativistic mean field (RMF) approach, the shears mechanism of magnetic rotation based on configuration $\pi h_{11/2}^2 \otimes \nu h_{11/2}^{-2}$ in ^{142}Gd is microscopically and self-consistently examined by investigating the aligning angular momenta of the valence nucleons.

Key words magnetic rotation, relativistic mean field, shears mechanism

PACS 21.60.Jz, 21.10.-k, 23.20.-g, 27.60.+j

1 Introduction

Magnetic rotation[1] is a hot topic and attracts significant attention in high spin physics, such as studies of backbending[2], super-deformed rotational bands[3], wobbling motion[4] and chiral phenomena[5].

This novel kind of rotation appears in spherical or weakly deformed nuclei, in which the magnetic dipole vector arose from few proton particles (holes) and few neutron holes (particles) in high-j orbitals, rotates around the total angular momentum vector. At the band head, the proton and neutron angular momenta are almost perpendicular. This coupling results in the total angular momentum which is tilted from the principal axes. With an increase of the rotational frequency, both the proton and neutron angular momenta align toward the total angular momentum. Consequently, the direction of the total angular momentum does not change so much and regular rotational bands are formed in spite of the fact that the density distribution of the nucleus is almost spherical or weakly deformed. These kinds of rotation are called magnetic rotation in order to distinguish from the usual collective rotation in well-deformed nuclei (called electric rotation)[1].

Following the experimental observation of magnetic property for ^{199}Pb in 1994[6], many results have been reported on the existence of the magnetic rotation in $A\sim 80$, $A\sim 100$, $A\sim 130$, and $A\sim 200$[7].

On the theoretical side, the description of the shears bands requires a model which goes beyond the one dimensional cranking. Namely, the rotating axis does not coincide with any principal axis of the atomic nucleus, which leads to the tilted axis cranking (TAC) model[8] and the discovery of the magnetic rotation[1]. The qualities of the TAC approximation have been discussed and tested in Ref.[9] with the particle rotor model(PRM) which has already led to a remarkable successful description on chiral doublets bands[5, 10, 11]. The three dimensional cranking RMF model was developed in 2000, it has been applied so far for the magnetic rotation band in ^{84}Rb due to its sophistication and time consuming[12]. At the same time, the non-relativistic mean field approach[13, 14] has been developed to investigate the magnetic rotation and chiral doublet bands as well although more efforts are need to improved the description for the electromagnetic transition. Recently, the two dimensional cranking RMF approach has been developed[15] in order to investigate the magnetic rotation. As an example, the magnetic dipole band DB1 in ^{142}Gd has been investigated by the new two dimensional crank-

Received 3 September 2008
* Supported by National Natural Science Foundation of China (10705004, 10435010, 10221003)
1) E-mail: jpeng@bnu.edu.cn

ing RMF approach, including the spectra, electromagnetic transition $B(\mathrm{M1})/B(\mathrm{E2})$ ratio, the relation between the rotational frequency and the angular momentum, the characteristic of magnetic rotation and the shears mechanism. In this paper, we will continue to examine the shears mechanism of band DB1 in ^{142}Gd via analyzing the alignment of angular momenta of the valence nucleons.

2 Formulation

The staring point of the RMF theory is the standard effective Lagrangian density constructed with the degrees of freedom associated with nucleon field ψ, two isoscalar meson fields σ and ω, the isovector meson field ρ, and the photon field A[16—19]:

$$\begin{aligned}\mathcal{L} = {} & \bar{\psi}[\mathrm{i}\gamma^{\mu}\partial_{\mu} - M] \\ & \bar{\psi}[-g_{\sigma}\sigma - g_{\omega}\gamma^{\mu}\omega_{\mu} - g_{\rho}\gamma^{\mu}\boldsymbol{\tau}\cdot\boldsymbol{\rho}_{\mu} - e\gamma^{\mu}\frac{1-\tau_3}{2}A_{\mu}]\psi + \\ & \frac{1}{2}\partial^{\mu}\sigma\partial_{\mu}\sigma - \frac{1}{2}m_{\sigma}^{2}\sigma^{2} - \frac{1}{3}g_{2}\sigma^{3} - \frac{1}{4}g_{3}\sigma^{4} - \\ & \frac{1}{4}\Omega_{\mu\nu}\Omega^{\mu\nu} + \frac{1}{2}m_{\omega}^{2}\omega_{\mu}\omega^{\mu} + \frac{1}{4}c_{3}(\omega_{\mu}\omega^{\mu})^{2} - \\ & \frac{1}{4}\boldsymbol{R}_{\mu\nu}\cdot\boldsymbol{R}^{\mu\nu} + \frac{1}{2}m_{\rho}^{2}\boldsymbol{\rho}_{\mu}\cdot\boldsymbol{\rho}^{\mu} - \\ & \frac{1}{4}F_{\mu\nu}F^{\mu\nu}, \qquad (1)\end{aligned}$$

where all the symbols have the same meaning as in Ref. [15].

The corresponding Dirac equation for nucleons and Klein-Gordon equations for mesons obtained with the mean field approximation are solved by the expansion method in terms of eigenfunctions of the three-dimensional deformed oscillator in Cartesian coordinates. The equation of motion for the photon field is solved using the standard Green's function method due to its long range. Since the Coriolis terms in the Dirac equation break time-reversal symmetry in the intrinsic frame it induces spatial components of the currents, while the Coriolis term for the meson fields is neglected.

Furthermore, there are also others question are solved in the present two dimensional cranking RMF code: 1) In order to identify the required orbits we therefore transform the wave functions from the Cartesian basis with the quantum number $|n_x n_y n_z \pm \mathrm{i}\rangle$ to a spherical basis with the quantum numbers $|\mathrm{nljm}\rangle$ using the techniques given in Refs.[20,21]. 2)In order to keep the same occupation during the increase of rotational frequency, the parallel-transport law is adopted to follow the single particle levels that change with the increase of rotational frequency; 3) The constrain on Q_{2-1} is introduced to keep the rotating frame according with the inertial principal axis frame; and so on. The detailed formalism and numerical techniques can be seen in Ref.[15] and references therein.

3 Results and discussion

In Ref.[15], the tilted axis cranking RMF calculations with either freezing the tilted angle $\theta = 45^{\circ}$ to save the computing time or the tilted angle self-consistently determined by minimizing the total Routhian have been performed respectively. Compared with the Skyrme-Hartree-Fock results, the energies for the band DB1 in ^{142}Gd as functions of the total angular momentum are much better reproduced in the tilted axis cranking RMF calculation. Adopting microscopic current for the calculation of the nuclear magnetic moment instead of the empirical formula used in the previous RMF calculation, the experimental ratio $B(\mathrm{M1})/B(\mathrm{E2})$ is reproduced well without introducing any attenuation factor. The shears mechanism for the band DB1 in ^{142}Gd are microscopically and self-consistently demonstrated by the orientation of proton and neutron's angular momenta.

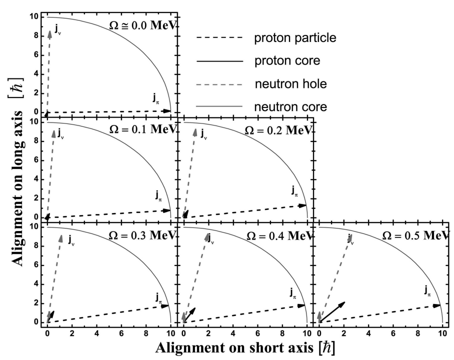

Fig. 1. The total angular momentum of the valence nucleons and of cores in two dimensional cranking RMF calculation with NL3, frozen $\theta = 45^{\circ}$ and the configuration $\pi h_{11/2}^{2} \otimes \nu h_{11/2}^{-2}$ for rotational frequencies $\Omega = 0.0, 0.1, ..., 0.5$ MeV are respectively given by black dash arrow, red dash arrow, black solid arrows(proton core), and red solid arrows(neutron core). Arc of radius $10\hbar$ is drawn in each panel.

In the present calculation, following the same procedures outlined in Ref.[15], we continue to examine the shears mechanism of band DB1 in ^{142}Gd by analyzing the alignment of angular momenta of the valence nucleons. We employ a spherical harmonic oscillator basis with 8 major shells for fermions and 20 shells for bosons. The effective interaction parameter sets NL3[22] and freezing the tilted angle $\theta=45^\circ$ have been used. The pairing correlations are not taken into account.

Here, the spins of the two valence neutron $h_{11/2}$ holes are defined as the spins of the two empty $h_{11/2}$ states, taken with the minus sign. To ensure that the total neutron spin is equal to the sum of the two holes' and the core's contributions, the core is defined as all the occupied neutron states plus the two empty $h_{11/2}$ states. The division of the proton single particle states into the two valence $h_{11/2}$ particles and the remaining core is obvious. So the length of the proton blade is the sum of the two $h_{11/2}$ valence proton's spin, and that of the neutron blade is the sum of the two $h_{11/2}$ valence neutron's spin, and they are given in Eqs.(2),(3):

$$\begin{cases} \boldsymbol{j}_\nu \equiv \boldsymbol{j}^n_{\text{blade}} = -\left(\boldsymbol{j}^n_{h_{11/2}\text{empty1}} + \boldsymbol{j}^n_{h_{11/2}\text{empty2}}\right) \\ \boldsymbol{j}_\pi \equiv \boldsymbol{j}^p_{\text{blade}} = +\left(\boldsymbol{j}^p_{h_{11/2}\text{occupy1}} + \boldsymbol{j}^p_{h_{11/2}\text{occupy2}}\right) \end{cases}, \quad (2)$$

$$\begin{cases} \boldsymbol{J}^\nu_{\text{core}} = \sum_i^{\text{N}} \boldsymbol{J}^n_i + (\boldsymbol{J}^n_{h_{11/2}\text{empty1}} + \boldsymbol{J}^n_{h_{11/2}\text{empty2}}) \\ \boldsymbol{J}^\pi_{\text{core}} = \sum_i^{P} \boldsymbol{J}^p_i - (\boldsymbol{J}^p_{h_{11/2}\text{occupy1}} + \boldsymbol{J}^p_{h_{11/2}\text{occupy2}}) \end{cases}. \quad (3)$$

The angular momentum of the valence nucleons $\boldsymbol{j}_\pi$, $\boldsymbol{j}_\nu$ and of cores (solid arrows) in two dimensional cranking RMF calculation with NL3, frozen $\theta = 45^\circ$ and the configuration $\pi h^2_{11/2} \otimes \nu h^{-2}_{11/2}$ in the plane spanned by the shortest and longest axes of the nucleus for rotational frequencies $\Omega = 0.0, 0.1, ..., 0.5$ MeV are shown in Fig.1. The results indicate that the angular momenta of the two $h_{11/2}$ proton particles (neutron holes) are nearly parallel. The two protons lying at the bottom of the $h_{11/2}$ shell will contribute angular momentum around 10 $\hbar$ along the short axis, while two neutron holes lying at the top of the $h_{11/2}$ shell will generate angular momentum around 10$\hbar$ aligning along the long axis. Namely, the length of proton and neutron blade given by black and red dash arrow in Fig.1 are approximate 10$\hbar$. At the bandhead, the proton and neutron blade are perpendicular to each other. This perpendicular orientation yields the total bandhead spin of about 14$\hbar$, and this is consistent with the results in Ref.[15]. The angular momenta of core is nearly zero. After the rotation is switched on, the two blades move towards each other. The alignment of angular momenta of the valence nucleons contributes the increase of the total angular momentum. In such a way, the shears mechanism for DB1 in ^{142}Gd is perfectly reproduced by the two dimensional cranking RMF calculation. Meanwhile one should note that the core generates its angular momentum for $\Omega > 0.30$ MeV because of the change of core structure. The detailed discussion could be found in Ref.[15].

4 Summary

In summary, the angular momentum of the valence nucleons and of cores are obtained using the new two dimensional cranking RMF calculation with NL3, frozen $\theta = 45^\circ$ and the configuration $\pi h^2_{11/2} \otimes \nu h^{-2}_{11/2}$. The shears mechanism for the band DB1 in ^{142}Gd are microscopically and self-consistently demonstrated by the orientation of valence proton and neutron's angular momenta.

References

1 Frauendorf S, MENG J, Reif J. Proceedings of the conference on physics from large γ-ray detector arrays. Edited by Deleplanque M A, California, Report LBL35687, 1994, vol.II
2 Johnson A, Ryde H, Sztarkier J. Phys. Lett. B, 1971, **34**: 605
3 Twin P J, Nyakó B M, Nelson A H et al. Phys. Rev. Lett., 1986, **57**: 811
4 Bohr A, Mottelson B R. Nuclear Structure, New York: Benjamin, 1975, Vol.II
5 Frauendorf S, MENG J. Nucl. Phys. A, 1997, **617**: 131
6 Neffgen M, Baldsiefen G, Frauendorf S et al. Nucl. Phys. A, 1995, **595**: 499
7 Amita, Jain A K, Singh B. Atomic Data and Nuclear Data Tables, 2000, **74**: 283
8 Frauendorf S. Nucl. Phys. A, 1993, **557**: 259c
9 Frauendorf S, MENG J. Z Phys. A, 1996, **356**: 263
10 PENG J, MENG J, ZHANG S Q. Phys. Rev. C, 2003, **68**: 044324
11 Koike T, Starosta K, Hamamoto I. Phys. Rev. Lett., 2004, **93**: 172502
12 Madokoro H, MENG J, Matsuzaki M, Yamaji S. Phys. Rev. C, 2000, **62**: 061301
13 Olbratowski P, Dobaczewski J, Dudek J et al. Acta Physica Polonica B, 2002, **33**: 389
14 Olbratowski P, Dobaczewski J, Dudek J, Płóciennik W. Phys. Rev. Lett., 2004, **93**(5): 052501-1
15 PENG J, MENG J, RING P, ZHANG S Q. Phys. Rev. C, **78**: 024313
16 Serot B D, Walecka J D. Adv. Nucl. Phys., 1986, **16**: 1
17 Reinhard P G. Rep. Prog. Phys., 1989, **52**: 439
18 Ring P. Prog. Part. Phys., 1996, **37**: 193
19 MENG J, Toki H, ZHOU S G et al. Prog. Part. Nucl. Phys., 2006, **57**: 470
20 Chasman R R, Wahlborn S. Nucl. Phys. A, 1967, **90**: 401
21 Talman J D. Nucl. Phys. A, 1970, **141**: 273
22 Lalazissis G A, König J, Ring P. Phys. Rev. C, 1997, **55**: 540